NÖHÜ Müh. Bilim. Derg. / NOHU J. Eng. Sci., 16 (2026), 1823182
Niğde Ömer Halisdemir Üniversitesi Mühendislik Bilimleri Dergisi
Niğde Ömer Halisdemir University Journal of Engineering Sciences
Araştırma makalesi / Research article
www.dergipark.org.tr/tr/pub/ngumuh / www.dergipark.org.tr/en/pub/ngumuh

Investigating the effects of fresh-state mechanics on early-age failure mechanisms in 3D concrete printing

3D beton yazdırmada taze hâl mekaniğinin erken yaş hasar mekanizmaları üzerindeki etkilerinin incelenmesi

Öznur Kocaer[1,*]

[1] *Hacettepe University, Faculty of Engineering, Department of Civil Engineering, 06800, Ankara, Türkiye*
[1] *The Scientific and Technological Research Council of Türkiye (TÜBİTAK), Ankara, Türkiye*

Abstract

A voxel-based finite element framework was employed to simulate fresh-state stability in extrusion-based 3D concrete printing. The model incorporated time-dependent material laws for Young's modulus and cohesion and activated voxels according to the actual deposition sequence, enabling realistic layer-by-layer build-up under gravity. Experimentally characterized printable mortars reported in the literature were used to investigate how rheological evolution influences deformation behavior, failure mechanisms, and achievable build height. The simulations showed that mixtures exhibiting rapid early-age stiffening and strong cohesion development provided higher load-bearing capacity but failed abruptly through elastic-type buckling once a critical state was reached. Mixtures with more gradual rheological evolution displayed smoother deformation and enhanced ductility, accompanied by lower build height. The equivalent stress–plastic strain response captured these contrasting regimes, linking sharp peaks to stiffness-dominated, brittle behavior and extended plateaus to viscoplastic accommodation. The findings highlight that optimal printability depends not solely on maximizing early strength but on synchronizing material evolution with deposition timing. The voxel-based activation strategy proved effective for predicting instability onset, stress localization, and collapse morphology using literature-derived rheology, offering a validated and open-source approach for pre-printing assessment and data-informed mixture and process design.

Keywords: 3D Concrete printing, Numerical modeling, Additive manufacturing, Material parameters, Fresh-state mechanics

Öz

Ekstrüzyon tabanlı 3B beton yazdırmada taze hâl stabilitesini modellemek amacıyla voksel tabanlı bir sonlu eleman çerçevesi kullanılmıştır. Model, Young modülü ve kohezyon için zamana bağlı malzeme yasalarını içermekte ve vokselleri gerçek yerleştirme sırasına göre etkinleştirerek, yerçekimi etkisi altındaki katmanlı inşa sürecini gerçeğe yakın şekilde yeniden üretmektedir. Literatürde deneysel olarak karakterize edilmiş baskıya uygun harçlar, reolojik evrimin şekil değiştirme davranışı, hasar mekanizmaları ve erişilebilir baskı yüksekliği üzerindeki etkisini incelemek için kullanılmıştır. Simülasyonlar, erken yaşta hızlı sertleşme ve yüksek kohezyon gelişimi gösteren karışımların daha yüksek yük taşıma kapasitesine ulaştığını, ancak kritik duruma gelindiğinde elastik tipte ani bir burkulma ile göçtüğünü ortaya koymuştur. Buna karşılık, reolojik özellikleri daha yavaş gelişen karışımlar daha düzgün bir deformasyon süreci ve artmış süneklik sergilemiş, ancak daha düşük baskı yüksekliğine ulaşabilmiştir. Eşdeğer gerilme–plastik şekil değiştirme tepkisi, bu iki rejim arasındaki farkları açıkça yansıtmış; keskin gerilme zirveleri rijitlik hâkimiyetindeki kırılgan davranışa, geniş plato bölgeleri ise viskoplastik uyuma karşılık gelmiştir. Bulgular, en uygun baskı yapılabilirliğinin yalnızca erken yaş dayanımının artırılmasına değil, aynı zamanda malzeme evriminin katman yerleştirme zamanlamasıyla uyumlu hâle getirilmesine bağlı olduğunu göstermektedir. Voksel tabanlı aktivasyon stratejisi, literatür kaynaklı reoloji kullanılarak kararsızlık başlangıcını, gerilme yığılmalarını ve çökme morfolojisini öngörmede etkili bulunmuş; baskı öncesi değerlendirme ve veri odaklı karışım ile proses tasarımı için doğrulanmış ve açık kaynaklı bir yaklaşım sunmuştur.

Anahtar kelimeler: 3D beton yazdırma, Nümerik modelleme, Eklemeli imalat, Malzeme parametreleri, Taze-hâl mekaniği

1 Introduction

Additive manufacturing (AM), commonly referred to as 3D printing, is rapidly emerging as a transformative technology in construction [1,2]. This not only advances a production technique to a higher level but also enables full automation of production and provides significant benefits such as a high degree of design freedom [3,4]. In practice, 3D printers enable architects and engineers to produce

* Sorumlu yazar / Corresponding author, e-posta / e-mail: oznurkocaer@hacettepe.edu.tr (Ö. Kocaer)
Geliş / Received: 13.11.2025 Kabul / Accepted: 26.12.2025 Yayımlanma / Published: 17.02.2026
doi: 10.28948/ngumuh.1823182

complex freeform geometries (e.g. curved facades or lattice structures) that would be very difficult or costly to achieve with conventional formwork [5]. This flexibility has been shown to slash construction costs: for example, Lloret et al. [6] report that eliminating traditional formwork via 3D printing can cut 35–60% of concrete construction costs. At the same time, remote-controlled printing systems reduce on-site labor and improve safety, since the machine handles heavy placement tasks. In fact, 3D-printed concrete has significant advantages over traditional concrete construction, offering substantial savings in formwork and labor costs [7]. By fabricating structures directly from digital models, 3D printing also integrates naturally with Building Information Modeling (BIM) and other digital planning tools [8], further enhancing precision and coordination in the construction process.

Beyond design and automation, 3D printing promises major sustainability gains. Because material is deposited only where needed, on-demand, waste generation is dramatically reduced. As indicated by De Schutter et al. [9], 3D concrete printing enables the efficient use of materials by precisely depositing concrete where needed, and even allows incorporation of recycled aggregates into the mix. Life-cycle assessments confirm these benefits: a 3D-printed wall could outperformed traditional construction in almost all environmental impact categories. A key reason is that printing requires no formwork or reinforcing steel, greatly lowering embodied energy and material use [10]. Notably, a comparative study found that a bathroom unit made by 3D printing achieved ~25% cost savings and an 85.9% reduction in CO_2 emissions versus a conventionally cast unit [11]. In addition, many studies have demonstrated that higher material efficiency and local sourcing in 3D printing can reduce transportation and waste disposal emissions [12-14]. In sum, 3D concrete printing aligns closely with global sustainability goals by minimizing waste and enabling greener materials (e.g. Alkali-activated binders) in building projects.

The combination of automation and precision also drives down labor and time demands. By automating repetitive tasks like layer dispensing, 3D printers shorten schedules and cut labor costs. Eliminating formwork not only saves material but also saves the heavy cost of formwork and labor [7]. Moreover, the ability to operate machines remotely (even in off-site factories or harsh environments) can further improve safety and productivity [15]. In practice, full-scale 3D-printed buildings have been realized with integrated BIM workflows and automated control to manage printing speed and geometry. Taken together, these advances imply that 3D printing can revolutionize construction by delivering unmatched design flexibility, higher efficiency, and lower lifecycle costs. Future work on large-scale systems, novel printable materials, and supportive regulations will further extend its impact [8,9].

Despite these promises, scaling 3D concrete printing from proof-of-concept to widespread practice requires deeper understanding of fresh-state behavior and structural integrity during printing. The mechanical performance of a printed object depends on many interrelated factors: the rheology and early-age hardening of the concrete, the geometry of each layer, the timing between layers, loading conditions, and potential defects or weak interfaces. Optimal settings for print speed, layer height, or mix design are often found by trial-and-error in experiments, which is slow and costly [16-18]. Mechanistic modeling is therefore essential to predict how printing parameters affect buildability and strength. To this end, researchers have recently coupled numerical simulation with laboratory data to analyze material deposition and stress development. For example, Suiker [19] introduced a wall-stability model that considers both elastic buckling and plastic yielding of 3D-printed walls. Similarly, another study relied on measured rheological properties together with the Mohr–Coulomb yield criterion, and the resulting model showed strong agreement with experiments across different layer configurations [20]. Wolfs et al. [21] developed a time-dependent finite-element model using a Mohr–Coulomb failure criterion and found that cohesion, stiffness and strength of the extruded concrete grow approximately linearly with age. These studies show that fresh-geometry and failure modes (e.g. global buckling, local yielding) can indeed be predicted, guiding safer design of 3D-printed elements.

Despite the significant progress achieved in recent studies on numerical modeling of 3D concrete printing, certain process–material interactions remain insufficiently represented in current frameworks. Existing models typically incorporate time-dependent rheological parameters [19,21], yet the deposition process is often idealized, and the link between actual layer-by-layer activation and the evolving fresh-state mechanical behavior is simplified or treated indirectly. As highlighted by Buswell et al. [4] and Wolfs et al. [21], accurately capturing the interplay between deposition sequence, rheological aging, and early-age load transfer is essential for predicting instability modes such as elastic buckling, plastic yielding, and shear localization. However, available modeling strategies still offer limited capability to evaluate how these coupled mechanisms govern stress redistribution and collapse onset under realistic printing conditions. Addressing this gap, the present study employs a voxel-based activation framework that explicitly synchronizes deposition timing with time-dependent mechanical evolution to examine fresh-state stability and failure mechanisms in extrusion-based 3D concrete printing.

Building on this foundation, the present study develops and validates a comprehensive voxel-based simulation workflow for extrusion 3D concrete printing. To this end, the open-source Concrete3DLab “VoxelPrint” plugin (a Grasshopper/Abaqus tool) coupled to the finite-element solver CalculiX [22] was employed. In this approach, every extruded strand is divided into small voxel elements, which are turned on at the precise time indicated by the G-code. The instantaneous material state (yield stress, cohesion, elastic stiffness, fracture energy, etc.) of each voxel is set by a time-dependent rheology model that accounts for hydration and aging. This allows each layer to build up strength in simulation just as it does in reality. The model was calibrated according to the experimental framework proposed by

Kocaer and Kul [23], ensuring consistency between numerical predictions and measured structural behavior. Following this calibration, the model was employed to perform collapse analyses based on the fresh-state mechanical characteristics of different 3D-printable mortar mixtures. This approach allowed the influence of time-dependent material properties, such as Young's modulus, Poisson's ratio, friction angle, cohesion, and density, on structural stability and failure mechanisms to be systematically examined. The selected material parameters were adopted from previously published works [24,25], each reporting optimally printable mortars validated through experimental characterization. Through this integration, the developed framework enabled a detailed evaluation of how variations in fresh-state behavior govern buildability, deformation response, and collapse performance during extrusion-based 3D concrete printing.

The novel contributions of this study can be summarized as follows. First, the proposed framework explicitly synchronizes voxel-level activation with the actual G-code deposition timeline, enabling a realistic representation of build-up, load transfer, and sequential stiffening during printing; this distinguishes the approach from existing finite-element models that typically rely on generalized layer activation procedures. Second, the model incorporates experimentally calibrated, time-dependent fresh-state parameters, such as Young's modulus, cohesion, friction angle, and Poisson's ratio, directly at the time each voxel is activated, allowing the mechanical evolution of the material to be reflected in real time. Third, the study evaluates collapse mechanisms for different printable mortars by using rheological data obtained from the literature, demonstrating that the framework can assess buildability without needing mixture-specific re-calibration. Fourth, the analysis is implemented entirely within an open-source workflow that combines Grasshopper-based voxelization with the CalculiX solver, providing a reproducible and adaptable alternative to proprietary FE platforms. Finally, the findings reveal that the relative progression rates of stiffness and cohesion govern early-age stability and failure modes, offering a mechanistic basis for synchronizing material evolution with process timing during extrusion-based 3D concrete printing.

2 Methodology

2.1 Numerical analysis

The numerical analysis was carried out using a Grasshopper-based setup previously introduced by Vantyghem et al. [22]. Their method provides a structured way to assess the printability of complex shapes by incorporating essential factors such as printing speed, layer height, geometric layout, and the evolving mechanical behavior of the material. The parametric setup was developed within the Rhinoceros–Grasshopper platform through the Concrete3DLab plugin, which enables the simulation of extrusion-based printing processes. This plugin enables the simulation of extrusion-based additive manufacturing using the VoxelPrint technique, in which the printed geometry is discretized into uniform volumetric elements known as voxels. Each voxel represents a perfect cubic eight-node brick element (C3D8), ensuring a direct one-to-one correspondence between the voxelized geometry and the finite element (FE) mesh. As all voxels are identical in size and uniformly distributed, traditional concerns such as mesh refinement, element distortion, or mesh-size sensitivity are completely avoided. The voxelization process produces a single monolithic part, in which all voxels are merged without requiring explicit contact definitions or bonding constraints between layers.

The step-by-step activation of voxels along the printing path removes the need for mesh-independence checks, since the build sequence itself dictates the process. In this setup, essential material characteristics—such as time-dependent Young's modulus, Poisson's ratio, cohesion, dilation angle, and internal friction angle—are included. Process-related parameters, including nozzle design, printing speed, and layer thickness, are also specified. The mechanical behavior of each voxel is updated as it matures, capturing the gradual stiffening of the concrete during hydration. Consecutive layers are linked through shared nodes in a single mesh, which means that the interfaces are implicitly treated as fully bonded. The interlayer behavior is therefore governed indirectly by the time-dependent reduction in strength and stiffness of newly deposited voxels relative to the older ones, rather than by explicit cohesive elements. This assumption simplifies the analysis while still capturing realistic variations in the structural response along the build height. The Grasshopper definition was implemented to automate parameter intake, G-code parsing, voxelization via Concrete3DLab, and export of layer-activation .inp files; printing kinematics (nozzle speed, layer height, bead width) were exposed as controllable inputs, while time stamps were mapped to voxel ages for assigning fresh state parameters at activation (Figure 1).

Collapse simulations were carried out in Abaqus to assess the structural stability of printed components under different operating conditions. The starting material parameters were taken from experimental data, and the influence of extrusion temperature was omitted. A time-dependent analysis was performed to track how the material properties evolved during printing [23]. The first printed layer was treated as a fixed support to maintain stability and ensure correct load transfer in the model. Each subsequent layer was introduced as a gradually applied load, allowing the material response and overall structural behavior to be examined in detail.

Using this method, collapse heights were identified for various printing setups, offering quantitative insight into the factors that lead to failure. The numerical outcomes were compared with the experimental findings of Wolfs and Suiker [26], and the close match between the two confirmed the reliability of the approach. The validation also demonstrated the model's ability to adapt to variations in geometry and nozzle configuration. Additional experimental validations and extended parametric analyses of a large-scale data set were presented in detail by Kocaer & Kul [23].

Building upon this validated framework, three distinct 3D-printable mortar mixtures characterized in previous studies [24,25] were incorporated into the numerical model to assess failure mechanisms under different material

conditions. For each mixture, experimentally determined fresh-state parameters, namely Young's modulus, Poisson's ratio, internal friction angle, dilation angle, cohesion, and density, were adopted to represent optimally printable mortars identified in the literature (Table 1). These datasets provided realistic input for simulating early-age mechanical behavior and enabled direct comparison among mixtures with differing rheological characteristics. Through this integration, collapse analyses were conducted to evaluate how variations in these fresh-state properties influence structural buildability, deformation behavior, and overall stability during the layer-by-layer printing process.

3 Results and discussions

The comparative numerical analysis of the mortars proposed by Nguyen-Van et al. [24] and Imran et al. [25] provides critical insight into how early-age rheological evolution controls the failure patterns of 3DCP structures. Although both systems were simulated under identical geometric and boundary conditions, their distinct time-dependent stiffness and cohesion characteristics produced fundamentally different deformation responses. As shown in Figure 2, stress propagation, localization, and collapse morphology varied considerably between the two materials, underscoring the decisive role of fresh-state mechanical evolution in the printability of cementitious composites.

The Nguyen-Van et al. [24] mixture demonstrated a rapid modulus build-up $E(t) = 0.06 \cdot t\,[\mathrm{MPa}]$ and strong cohesion increase $c(t) = 3.2 \cdot t\,[\mathrm{kPa}]$, leading to high early rigidity and a correspondingly brittle collapse mechanism. The stress distribution remained largely vertical and symmetric during the initial printing stages, indicating efficient load transfer between layers.

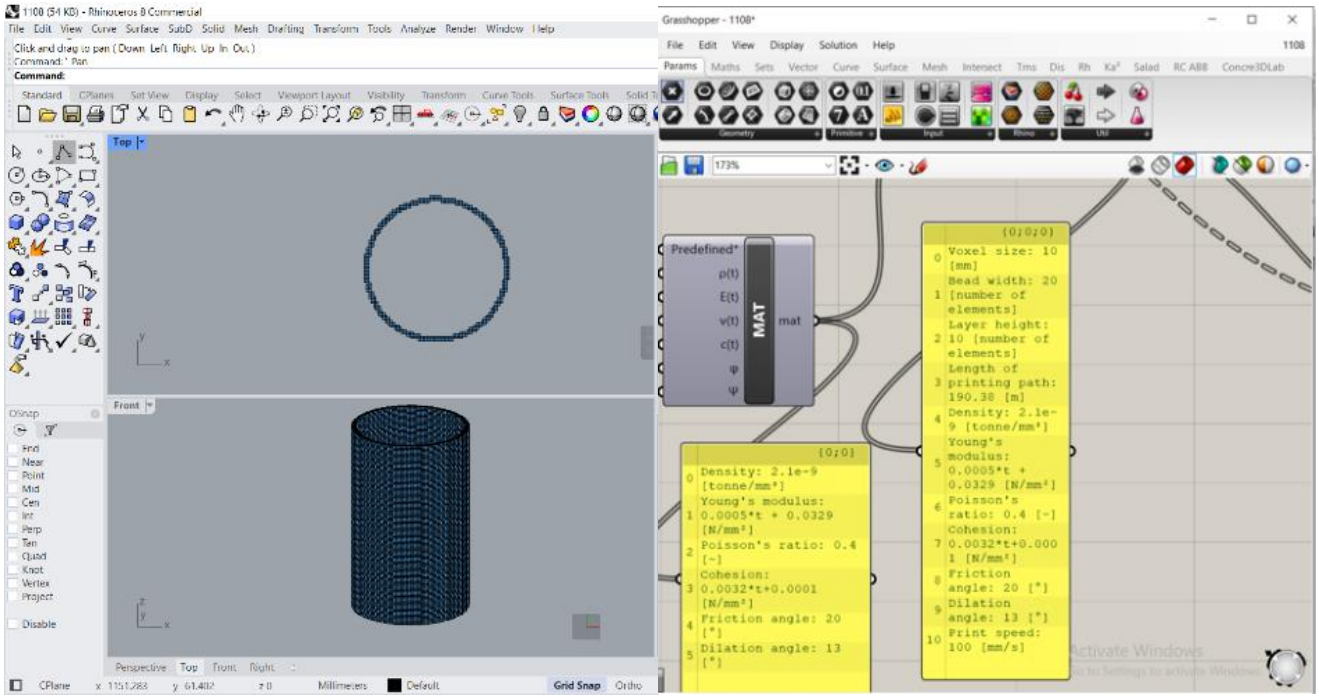

Figure 1. Overview of the voxel-based simulation workflow. The panel on the left displays the voxelized cylindrical wall generated in Rhinoceros, where each voxel corresponds to a C3D8 solid element used in the finite element analysis. The panel on the right presents the Grasshopper workflow responsible for reading G-code, mapping deposition timestamps to voxel ages, and applying time-dependent material properties.

Table 1. Fresh state paramaters of 3D-printable mortars and printing parameters

Fresh State Properties	Nguyen-Van et al. [24]	Imran et al. [25]
Young's Modulus, E(t[min])	0.06·t [MPa]	0.5·t+32.9 ·t [kPa]
Poisson Ratio, ν	0.30	0.40
Dilation Angle, ψ	13	13
Friction Angle, ϕ	20	0.1074 t +54.439
Cohesion, c(t[min])	3.2·t [kPa]	0.02538·t+5.153 [kPa]
Density, ρ	2.066E-9 (ton/mm3)	2.183E-9 (ton/mm3)
Printing Parameters for Numerical Simulations		
Wall radius, r	0.3 (m)	
Layer thickness, h	20.0 (mm)	
Height of individual layer, tI	10 (mm)	
Velocity of printer head, vn	100 (mm/s)	

However, once the gravitational stress exceeded the critical elastic threshold, the structure lost stability abruptly through upward-propagating buckling bands near the upper region. This response typifies a stiffness-dominated system where the rate of modulus growth outpaces the development of interlayer bonding. In such cases, strain energy accumulates rapidly without sufficient viscous relaxation, producing sudden geometric failure. Similar phenomena have been observed experimentally by Suiker [19] and Wolfs et al. [21].

By contrast, the Imran et al. [25] mixture exhibited a more gradual and adaptive response. The higher Poisson ratio (0.40) and moderate stiffness evolution $E(t) = 0.5 \cdot t + 32.9 \cdot t$ [kPa] promoted partial lateral expansion and better stress redistribution, allowing the structure to accommodate deformation through controlled plastic flow. Yield initiation occurred progressively at mid-height, and the collapse developed via a combination of elastic compression and plastic shear localization rather than a single catastrophic event. This gradual deformation behavior is particularly desirable in large-scale printing, as it enables redistribution of stresses that arise from layer-height irregularities or local heterogeneity. Numerical and experimental research by Kruger et al. [20] and Xiao et al. [27] similarly demonstrated that mixtures with balanced rheological evolution maintain stability longer by facilitating gradual transition from viscoelastic to plastic regimes.

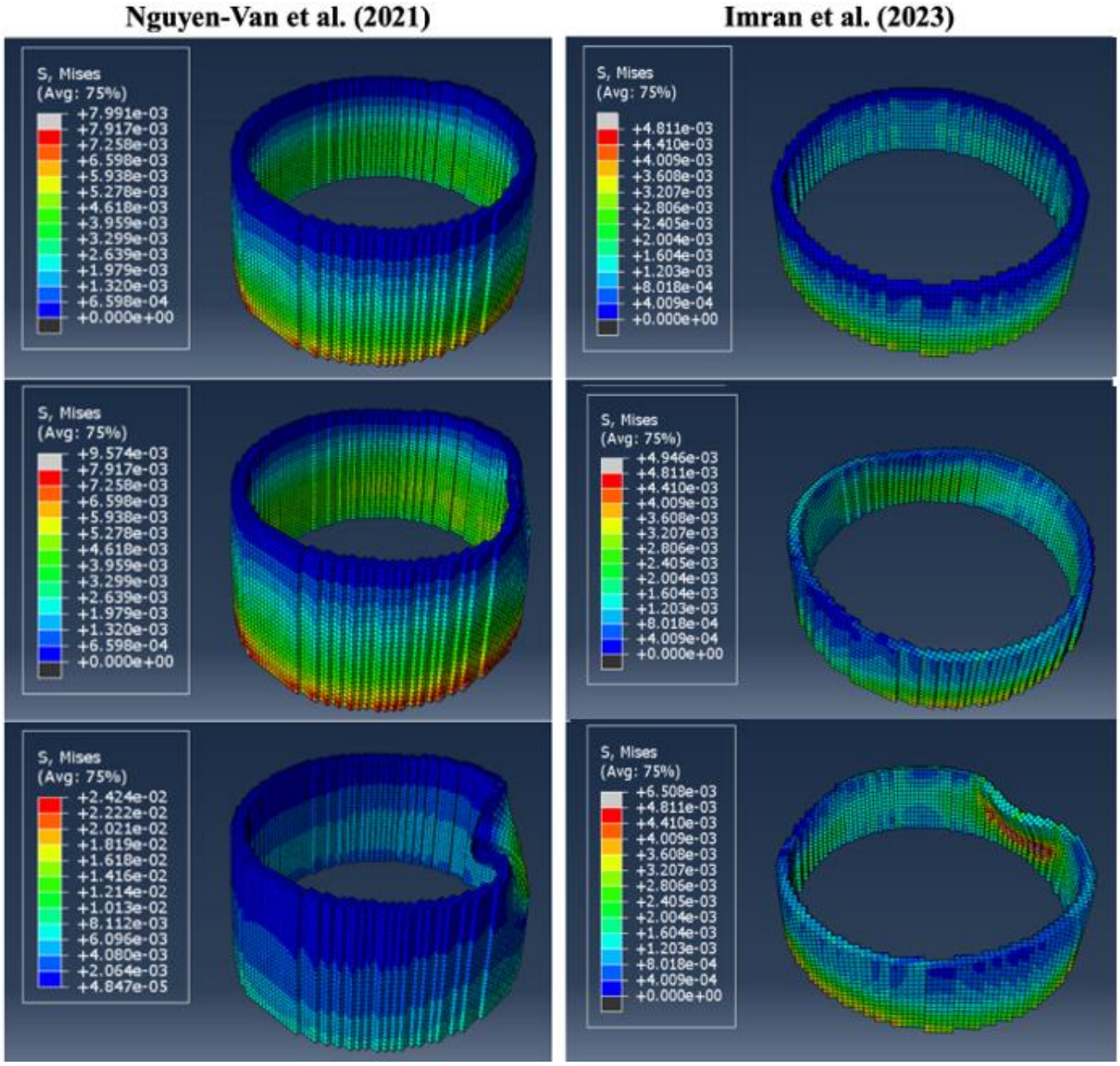

Figure 2. Numerical von Mises stress distributions for the two printable mortars examined. Left: Nguyen-Van et al. (2021); right: Imran et al. (2023). Rows represent successive printing stages showing the development of stress localization and collapse patterns.

The equivalent stress–plastic strain responses shown in Figure 3 further confirm the fundamental difference in the mechanical character of the two mortars. The Nguyen-Van mixture shows a sharp stress peak followed by an immediate decline, a hallmark of brittle materials with limited post-yield ductility. Conversely, the Imran mixture exhibits a smoother rise to a stress plateau at approximately 0.002 MPa, followed by gradual softening. This indicates a capacity for post-yield energy absorption and partial strain recovery, consistent with viscoplastic deformation behavior. Similar relationships between the rate of stiffening and the shape of the S, Mises–PEEQ curve were also established by Comminal et al. [16] and Reinold et al. [17], confirming that time-dependent modulus growth governs the transition from elastic to plastic flow in freshly printed layers.

In quantitative terms, the Nguyen-Van et al. [24] mixture attained a higher maximum build height prior to collapse than the Imran et al. [25] mixture, indicating superior buildability despite its brittle failure signature. This outcome is consistent with its faster early-age stiffening and stronger cohesion growth, which together enhanced self-weight resistance across successive layers. The contrasting behavior substantiates the stiffness-versus-ductility trade-off described in prior studies: systems optimized for rapid structural build-up can achieve greater height but are susceptible to abrupt elastic buckling once the critical limit is reached, whereas mixtures with more moderate stiffening permit controlled deformation at the expense of ultimate height capacity [19-21].

From a mechanistic standpoint, these results indicate that faster modulus growth E(t) raises the critical build height but reduces post-critical ductility. Consequently, the Nguyen-Van [24] system achieves higher storeys before failure yet collapses suddenly once the critical state is reached, exhibiting high sensitivity to imperfections. In contrast, steady cohesion growth c(t) and interlayer friction in the Imran system provide lateral constraint, enabling gradual stress redistribution and delaying catastrophic collapse, albeit at a lower attainable height. Thus, the balance between the rates of E(t) and c(t) emerges as a governing design indicator [9,28].

The results also provide practical implications for printing process control. In rapidly stiffening systems, shorter interlayer intervals are essential to maintain adhesion and prevent cold joints, since the material transitions to a load-bearing state almost immediately after extrusion. For materials with slower stiffening but sustained cohesion development, longer printing cycles may be tolerated, offering flexibility for complex geometries and extended printing times. This behavior resonates with the rheology–process interdependence discussed by Nguyen-Van et al. [24] and Kazemian et al. [15], who highlighted the need for coupling real-time rheological feedback with layer-deposition control.

The voxel-based simulation approach employed in this study successfully captured these mechanisms in a time-resolved manner. Unlike traditional element-activation models, the voxel strategy directly integrates time-dependent material parameters at each printing increment, enabling accurate tracking of stress redistribution, softening, and collapse onset. The numerical predictions reproduced the failure morphologies observed in experimental investigations, thereby confirming the validity of this mechanistic modeling framework.

The data presented in Table 2 indicate that the mechanical performance of the mixtures in their fresh state differs considerably between the two studies. The higher maximum equivalent stress reported by Nguyen-Van et al. [24] (0.025 MPa), compared with the substantially lower value reported by Imran et al. [25] (0.007 MPa), suggests that the former mixture develops a more robust load-bearing capacity at early age. Likewise, the plastic deformation capacity (PEEQ), which reaches 0.23 in the Nguyen-Van mixture but remains at 0.11 in the Imran mixture, demonstrates that the resistance to deformation beyond the yield point varies significantly. These distinctions underscore that early-age ductility and deformation tolerance are critical factors governing the structural stability of printed layers in 3D concrete printing.

The difference in critical collapse height further reinforces these findings. The Nguyen-Van mixture remains stable up to 310 mm, indicating a higher degree of stiffness and structural integrity in its fresh state, whereas the Imran mixture loses stability at 140 mm, reflecting a more limited early-age rigidity. Collectively, these results show that variations in early-age mechanical performance, particularly load-bearing capacity, deformation tolerance, and stability, play a decisive role in ensuring reliable geometry retention during the additive manufacturing process.

Overall, the comparison between Nguyen-Van et al. [24] and Imran et al. [25] demonstrates that optimizing 3D-printable mortars is not simply a matter of increasing stiffness or yield strength, but rather achieving the correct synchronization between material evolution and process timing. The capacity of a printed structure to resist gravity-induced deformation depends on how rheological properties evolve relative to the deposition rate, a dynamic balance that ultimately defines the buildability window. The results substantiate that predictive modeling, when grounded in experimentally derived rheological data, can serve as a powerful design tool to pre-empt failure, refine printing parameters, and accelerate the adoption of additive construction for large-scale applications.

Table 2. Key numerical results for the two printable mortars

Fresh State Properties	Nguyen-Van et al. [24]	Imran et al. [25]
Maximum equivalent stress (MPa)	0.025	0.007
Plastic strain capacity, PEEQ (–)	0.23	0.11
Critical collapse height (mm)	310	140

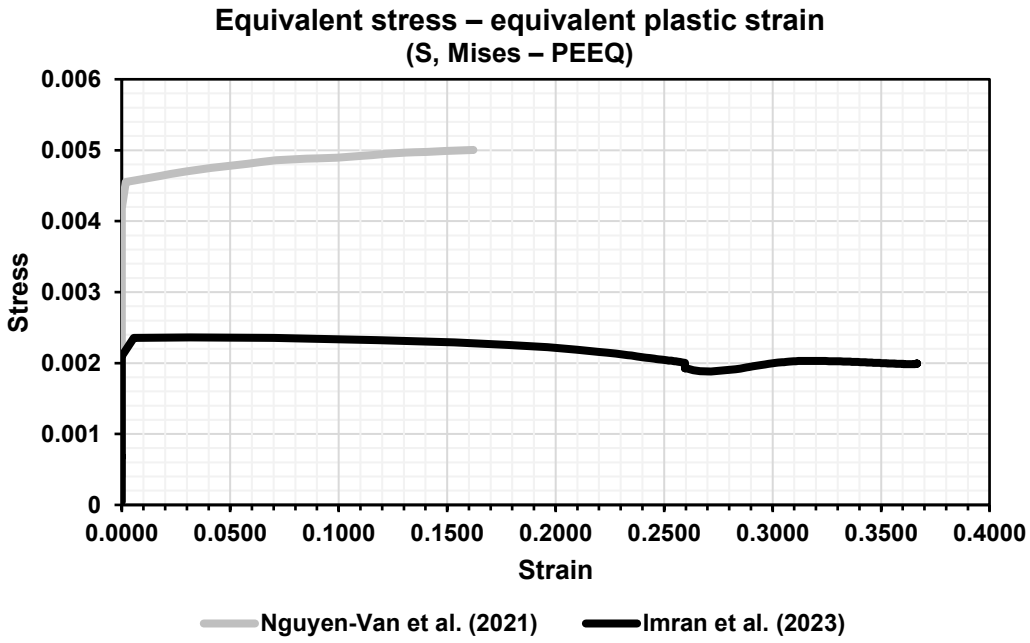

Figure 3. Equivalent stress-equivalent plastic strain results of 3D-printable mortars

4 Conclusion

The primary aim of this study was to develop a voxel-based numerical framework capable of representing the time-dependent fresh-state mechanical behavior of extruded concrete during layer-by-layer printing. By integrating real deposition timing with evolving rheological parameters, the study sought to evaluate how material stiffening, cohesion growth, and frictional resistance collectively govern early-age stability, stress redistribution, and collapse mechanisms. With this objective, the research provides a structured and predictive approach for assessing buildability in extrusion-based 3D concrete printing, offering a mechanistic understanding of how material evolution interacts with process timing. The main outcomes of this research can be outlined as follows:

The mortar reported by Nguyen-Van et al. [24] reached a higher maximum build height, attributable to rapid early-age stiffening coupled with strong cohesion growth; failure, however, manifested abruptly as a stiffness-dominated elastic buckling once the critical state was reached.

The mortar reported by Imran et al. [25] developed stability more gradually; cohesion and friction furnished lateral constraint and stress redistribution, producing controlled, ductile collapse at a lower attainable height.

Printability is governed by the relative rates of E(t) and c(t) with respect to the deposition timeline, not by early strength alone; faster modulus growth raises critical height but reduces post-critical ductility, whereas steady cohesion growth enhances interlayer transfer and delay of catastrophic failure.

Interlayer timing must be synchronized with rheology, fast-setting systems benefit from shorter intervals to preserve bonding and avoid premature elastic buckling; slower-stiffening mortars with sustained cohesion can tolerate longer cycles and greater geometric complexity at the expense of ultimate height.

5 Future research recommendations

It is recommended that time-dependent stiffening and structuration in geopolymers be increased without sacrificing pumpability by optimizing activator chemistry (silicate/sodium ratio, modulus), water–activator ratio, and the use of benign accelerators. A denser granulometry (tailored PSD with supplementary fines or metakaolin content) should be pursued to raise early elastic modulus and yield stress. Packing models can be coupled with the voxel-activation simulations to target a minimum required E(t)-c(t) envelope for a given print rate. To compensate for lower fresh cohesion in geopolymers, shorter interlayer times, mild surface activation (e.g., light misting with dilute activator), and fresh-on-fresh deposition should be prioritized. Where permissible, thin interlayer primers compatible with alkali activation may be explored to increase c(t) at the interface.

Conflict of interest

The authors declare that there is no conflict of interest.

Similarity (iThenticate): 10%

References

[1] N. Labonnote, A. Rønnquist, B. Manum ve P. Rüther, Additive construction: state-of-the-art, challenges and opportunities. Automation in Construction, 72, 347–366, 2016. https://doi.org/10.1016/j.autcon.2016.08.026.

[2] S. H. Ghaffar, J. Corker ve M. Fan, Additive manufacturing technology and its implementation in construction as an eco-innovative solution. Automation in Construction, 93, 1–11, 2018. https://doi.org/10.1016/j.autcon.2018.05.005.

[3] T. A. M. Salet, F. P. Bos, R. J. M. Wolfs ve Z. Y. Ahmed, 3D concrete printing – a structural engineering perspective. Proc. 2017 fib Symposium: High Tech Concrete: Where Technology and Engineering Meet, Springer, xliii–lvii, 2017.

[4] R. A. Buswell, W. L. De Silva, S. Z. Jones ve J. Dirrenberger, 3D printing using concrete extrusion: a roadmap for research. Cement and Concrete Research, 112, 37–55, 2018. https://doi.org/10.1016/j.cemconres.2018.05.006.

[5] S. Lim, R. A. Buswell, P. J. Valentine, D. Piker, S. A. Austin ve X. De Kestelier, Modelling curved-layered printing paths for fabricating large-scale construction components. Additive Manufacturing, 12(Part B), 216–230, 2016. https://doi.org/10.1016/j.addma.2016.06.004.

[6] E. Lloret, A. R. Shahab, M. Linus, R. J. Flatt, F. Gramazio, M. Kohler, vd., Complex concrete structures: merging existing casting techniques with digital fabrication. Computer Aided Design, 60, 40–49, 2015. https://doi.org/10.1016/j.cad.2014.02.011.

[7] Y. Han, Z. Yang, T. Ding ve J. Xiao, Environmental and economic assessment on 3D printed buildings with recycled concrete. Journal of Cleaner Production, 278, 123884, 2021. https://doi.org/10.1016/j.jclepro.2020.123884.

[8] A. Paolini, S. Kollmannsberger ve E. Rank, Additive manufacturing in construction: a review on processes, applications, and digital planning methods. Additive Manufacturing, 30, 100894, 2019. https://doi.org/10.1016/j.addma.2019.100894.

[9] G. De Schutter, K. Lesage, V. Mechtcherine, V. N. Nerella, G. Habert ve I. Agusti-Juan, Vision of 3D printing with concrete—technical, economic and environmental potentials. Cement and Concrete Research, 112, 25–36, 2018. https://doi.org/10.1016/j.cemconres.2018.06.001.

[10] H. Alhumayani, M. Gomaa, V. Soebarto ve W. Jabi, Environmental assessment of large-scale 3D printing in construction: a comparative study between cob and concrete. Journal of Cleaner Production, 270, 122463, 2020. https://doi.org/10.1016/j.jclepro.2020.122463.

[11] Y. Weng, M. Li, S. Ruan, T. N. Wong, M. J. Tan, K. L. O. Yeong ve S. Qian, Comparative economic, environmental and productivity assessment of a concrete bathroom unit fabricated through 3D printing and a precast approach. Journal of Cleaner Production, 261, 121245, 2020. https://doi.org/10.1016/j.jclepro.2020.121245.

[12] O. Kocaer ve A. Aldemir, Confined compressive stress–strain model for rectangular geopolymer reinforced concrete members. Structural Concrete, 26(4), 4334–4347, 2025. https://doi.org/10.1002/suco.202300973.

[13] O. Kocaer ve A. Aldemir, Compressive stress–strain model for the estimation of the flexural capacity of reinforced geopolymer concrete members. Structural Concrete, 24(4), 5102–5121, 2023. https://doi.org/10.1002/suco.202200914.

[14] A. Kul, O. Kocaer, A. Aldemir, G. Yildirim ve S. S. Lucas, 3D printable one-part alkali-activated mortar derived from brick masonry wastes. Case Studies in Construction Materials, 21, e04081, 2024. https://doi.org/10.1016/j.cscm.2024.e04081.

[15] A. Kazemian, X. Yuan, O. Davtalab ve B. Khoshnevis, Computer vision for real-time extrusion quality monitoring and control in robotic construction. Automation in Construction, 2019. https://doi.org/10.1016/j.autcon.2019.01.022.

[16] R. Comminal, W. Silva, T. Andersen, H. Stang ve J. Spangenberg, Modelling of 3D concrete printing based on computational fluid dynamics. Cement and Concrete Research, 138, 106256, 2020. https://doi.org/10.1016/j.cemconres.2020.106256.

[17] J. Reinold, V. Nerella, V. Mechtcherine ve G. Meschke, Extrusion process simulation and layer shape prediction during 3D-concrete-printing using the particle finite element method. Automation in Construction, 2022. https://doi.org/10.1016/j.autcon.2022.104173.

[18] O. Bouzaglou, O. Golan ve N. Lachman, Process design and parameters interaction in material extrusion 3D printing: a review. Polymers, 15, 2280, 2023. https://doi.org/10.3390/polym15102280.

[19] A. Suiker, Mechanical performance of wall structures in 3D printing processes: theory, design tools and experiments. International Journal of Mechanical Sciences, 137, 145–170, 2018. https://doi.org/10.1016/j.ijmecsci.2018.01.010.

[20] J. Kruger, S. Zeranka ve G. Zijl, 3D concrete printing: a lower bound analytical model for buildability performance quantification. Automation in Construction, 106, 102904, 2019. https://doi.org/10.1016/j.autcon.2019.102904.

[21] R. Wolfs, F. Bos ve T. Salet, Early age mechanical behaviour of 3D printed concrete: numerical modelling and experimental testing. Cement and Concrete Research, 106, 103–116, 2018. https://doi.org/10.1016/j.cemconres.2018.02.001.

[22] G. Vantyghem, T. Ooms ve W. De Corte, VoxelPrint: a Grasshopper plug-in for voxel-based numerical simulation of concrete printing. Automation in Construction, 122, 103469, 2021. https://doi.org/10.1016/j.autcon.2020.103469.

[23] O. Kocaer and A. Kul, Parametric analysis of design and operational parameters in 3D concrete printing of wall elements. Journal of Building Engineering, 114494, 2025. https://doi.org/10.1016/j.jobe.2025.114494.

[24] V. Nguyen-Van, B. Panda, G. Zhang, H. Nguyen-Xuan ve P. Tran, Digital design computing and modelling for 3D concrete printing. Automation in Construction, 123, 103529, 2021. https://doi.org/10.1016/j.autcon.2020.103529.

[25] R. Imran, A. Al Rashid, S. A. Khan, H. Ilcan, O. Sahin, M. Sahmaran ve M. Koç, Buildability analysis on squared profile structure in 3D concrete printing (3DCP). European Journal of Materials, 3(1), 2276443,

2023. https://doi.org/10.1080/26889277.2023.2276443.

[26] R. J. M. Wolfs, A. S. J. Suiker, Structural failure during extrusion-based 3D printing processes. The International Journal of Advanced Manufacturing Technology, 104, 1, 565-584, 2019.

[27] J. Xiao, G. Ji, Y. Zhang, G. Ma, V. Mechtcherine, J. Pan ve S. Du, Large-scale 3D printing concrete technology: current status and future opportunities. Cement and Concrete Composites, 122, 104115, 2021. https://doi.org/10.1016/j.cemconcomp.2021.104115.

[28] M. Biehler, D. Lin, R. Mock ve J. Shi, 4DYNAMO: analyzing and optimizing process parameters in 4D printing for dynamic 3D shape morphing accuracy. Journal of Manufacturing Science and Engineering, 2024. https://doi.org/10.1115/1.4066222.